

# Measurement and Analysis of Visible Line Spectra with Inhomogeneous Spatial Distribution in LHD

H. YAMAZAKI, M. GOTO<sup>1)</sup>, S. MORITA<sup>1)</sup>, T.H. WATANABE<sup>1)</sup>  
and LHD experimental group

*Department of Fusion Science, School of Physical Science, Graduate University for Advanced Studies,  
Toki 509-5292, Gifu, Japan*

<sup>1)</sup>*National Institute for Fusion Science, Toki 509-5292, Gifu, Japan*

(Received 4 December 2006 / Accepted 30 March 2007)

Spatially resolved spectra have been measured with visible spectroscopy in Large Helical Device (LHD). Strong line emissions of H I, He I and C III have been observed at a limited area near the inboard-side X-point. Such a poloidally inhomogeneous radiation structure is drastically changed when the radius of the magnetic axis is shifted from  $R_{ax} = 3.6$  m to 3.9 m: another strong emission emerges near the outboard-side X-point. In order to understand the physical mechanism the electron temperature and density are evaluated from intensity ratios of neutral hydrogen and helium lines at poloidal locations near both the X-points and at the bottom O-point edge. It is found that the changes of the electron temperature and density along the poloidal direction are too moderate to explain the inhomogeneity of line emissions for both the configurations. The present result suggests that the poloidal inhomogeneity of neutral emissions arises owing to the inhomogeneous neutral density distribution rather than the difference of the electron density or temperature.

© 2007 The Japan Society of Plasma Science and Nuclear Fusion Research

Keywords: visible spectra, inhomogeneous profile, H $\alpha$ , He I, line intensity ratio

DOI: 10.1585/pfr.2.S1115

## 1. Introduction

It is well known that the plasma confinement is strongly influenced by neutral density near the plasma boundary. Since the plasma figure and the vacuum vessel of the Large Helical Device (LHD) have three-dimensionally complicated structures, the study of the neutral density distribution becomes more important. Then, the poloidal distribution of the neutrals has been extensively studied in LHD. Two-dimensional distribution of helium neutral line intensity has been recently determined with the help of Zeeman splittings in  $R_{ax} = 3.6$  m, where  $R_{ax}$  means a major radius position of magnetic axis [1]. As a result, it is found that the intensity around the inboard-side X-point is much higher than other locations. Since the line intensity is a function of the electron temperature and density as well as the atomic density, determination of the former two parameters is necessary in order to evaluate the poloidal distribution of the neutral density. In this paper the parameter evaluation is attempted using intensity ratios among three neutral helium lines and two neutral hydrogen lines. On the other hand, the inhomogeneous distribution of the visible lines is drastically changed when the magnetic configuration is shifted outwardly. Another location of the strong line emission is also found near the outboard-side X-point in addition to that near the inboard-side X-point. The plasma parameters at the emission locations are

determined for the two different magnetic configurations and the relationship between the line intensity and the neutral density is discussed.

## 2. Experimental Setup

Figure 1 shows the plasma cross section and viewing chords for the present observation. The line emissions in the visible and UV wavelength ranges are observed with 26 optical fibers having a core diameter of 100  $\mu$ m. The line-of-sight is collimated with a lens and thus the spatial resolution of 30 mm is obtained at the plasma center. The emissions are transferred to a 50 cm visible spectrometer equipped with a 100 grooves/mm grating. A CCD (charge coupled device) having the detection area of  $26.6 \times 6.6$  mm<sup>2</sup> (1024  $\times$  256 channels, 26  $\mu$ m  $\times$  26  $\mu$ m/pixel) is used as the detector. The wavelength range of 300 nm to 800 nm has been simultaneously measured with a time resolution of 200 ms.

Figure 2 shows an example of the spectra measured with the line-of-sight at  $z = 0.04$  m for helium discharge. In LHD, many efforts have been made for the wall conditioning using He- and Ar-glow discharges in addition to the boronization, since the wall temperature for baking is limited below 95 °C. Only carbon is recently a dominant impurity because the divertor plates are made of carbon composite [2]. Actually, the C III line (464.7 nm) designated in Fig. 2 is always clearly observed with relatively

author's e-mail: yamazaki.hisamichi@lhd.nifs.ac.jp

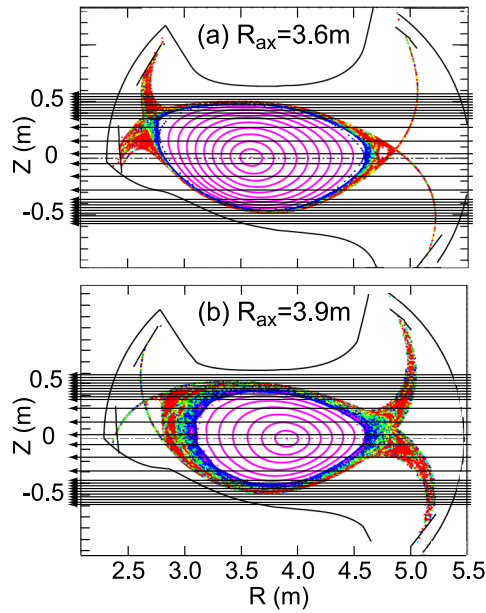


Fig. 1 Horizontally elongated cross section of LHD plasma in (a)  $R_{ax} = 3.6$  m and (b) 3.9 m with 26 view chords for visible spectroscopy.

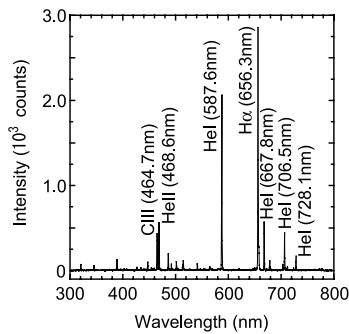


Fig. 2 Visible spectrum in helium plasma at central sightline ( $z = 0.04$  m) in  $R_{ax} = 3.6$  m.

strong intensity.

### 3. Experimental Results and Discussions

Figure 3(a) shows the vertical distribution of H I (656.3 nm), He I (667.8 nm) and C III (464.7 nm) intensities observed from  $R_{ax} = 3.6$  m discharge (also see Fig. 1 (a)) with helium gas.

Strong emissions are observed at  $z = 0.38$  m for all the three lines. In addition, another peak also appears at  $z = 0.5$  m and may arise from line-integral effect due to the relatively long line-of-sight at the plasma edge (see Fig. 1). These peaks also appear in Fig. 5 with smaller intensity but not outstanding. When the He I distribution in Fig. 3 (b) is compared with the 2-dimensional structure of helium neutral emissions seen in Ref. [1], it can be easily understood that these emissions are mainly dominated from the vicin-

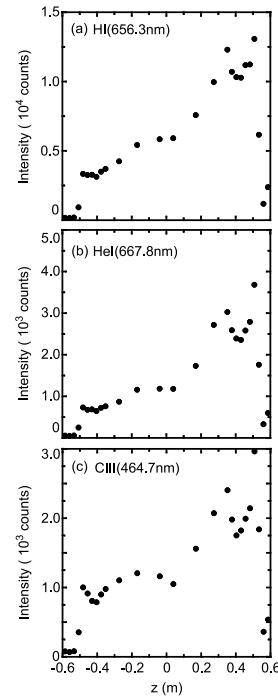


Fig. 3 Spatial distribution of (a) H I (656.3 nm), (b) He I (667.8 nm) and (c) C III (464.7 nm) in  $R_{ax} = 3.6$  m discharge.

Table 1 Local  $T_e$  and  $n_e$  evaluated from line ratios of He I  $I(667.8 \text{ nm})/I(728.1 \text{ nm})$ , He I  $I(728.1 \text{ nm})/I(706.5 \text{ nm})$  and H I  $I(656.3 \text{ nm})/I(434.1 \text{ nm})$  in  $R_{ax} = 3.6$  m.

$z$	HeI ratio ( $I(728.1 \text{ nm})/I(706.5 \text{ nm})$ )	$T_e$ (eV)	HeI ratio ( $I(667.8 \text{ nm})/I(728.1 \text{ nm})$ )	$n_e$ ( $10^{18} \text{ m}^{-3}$ )
(Inboard x-point) $z=0.38$ m	0.43	60	1.94	1.8
(outboard x-point) $z=-0.17$ m	0.43	50	3.01	4.2
(bottom O-point) $z=-0.48$ m	0.58	75	3.11	5.0

$z$	HI ratio ( $I(656.3 \text{ nm})/I(434.1 \text{ nm})$ )	$n_e$ ( $10^{18} \text{ m}^{-3}$ )
(Inboard x-point) $z=0.38$ m	32.6	2.8
(outboard x-point) $z=-0.17$ m	33.1	3.0
(bottom O-point) $z=-0.48$ m	42.7	5.0

ity of the inboard-side X-point.

The evaluation of  $T_e$  (electron temperature) and  $n_e$  (electron density) is attempted at each line-of-sight to investigate the contribution of these parameters to the formation of inhomogeneous poloidal distribution. A set of three He I emissions is used for the parameter measurement [3, 4]. According to Ref. [4], the intensity ratios of  $I(667.8 \text{ nm})/I(728.1 \text{ nm})$  and  $I(728.1 \text{ nm})/I(706.5 \text{ nm})$  are dominantly sensitive to  $n_e$  and  $T_e$ , respectively. We derive these intensity ratios from the observed spectra at  $z = 0.38$  m (near the inboard-side X-point),  $-0.17$  m (near the outboard-side X-point) and  $-0.48$  m (at the bottom-side O-point) as shown in Table 1. Here, it is seen from Ref. [1] that the line-of-sight at  $z = -0.17$  m is dominated by emissions near the outboard-side X-point. The depen-

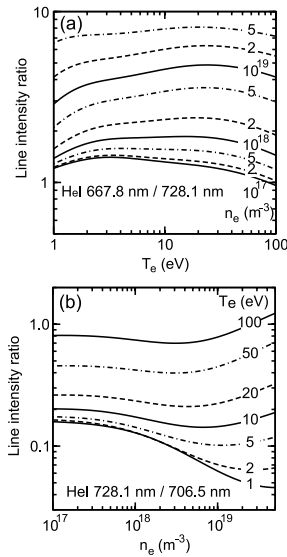


Fig. 4 Line intensity ratios of (a) He I  $I(667.8 \text{ nm})/I(728.1 \text{ nm})$  and (b) He I  $I(667.8 \text{ nm})/I(728.1 \text{ nm})$  calculated from C-R model simulation.

dence of those intensity ratios on  $T_e$  and  $n_e$  is calculated with a collisional-radiative model (C-R model) [4] and results are shown in Fig. 4.

The ratio weakly depends on  $T_e$  and is sensitive to  $n_e$  for  $I(667.8 \text{ nm})/I(728.1 \text{ nm})$  and vice versa for  $I(728.1 \text{ nm})/I(706.5 \text{ nm})$ . The parameters  $T_e$  and  $n_e$  at the emission locations can be thus determined from those ratios. Results are also listed in Table 1.

The value of  $n_e$  around the inboard-side X-point is approximately half as compared to that around the outboard-side X-point, while  $T_e$  is similar for both the locations. Since the He I emission intensity around the inboard-side X-point is about 2 times higher than that around the outboard-side X-point, the helium neutral density around the inboard-side X-point is estimated about 4 times higher than that around the outboard-side X-point. The  $n_e$  is considerably higher at the bottom-side O-point than around both X-points. The ergodic layer thickness is much thinner at the O-point than at the X-points. If the penetration depth of the helium neutrals is the same for all the poloidal location, the helium emissions from the O-point occur at deeper radial positions, namely, at locations having higher  $n_e$  and  $T_e$ . Anyway, we clearly understand that helium neutrals are much low at the O-point as compared to around the X-points.

The ion flux distribution on the helically located divertor plates has been measured by Langmuir probes showing a poloidally inhomogeneous distribution [5,6]. A large nonuniform ion flux on the inboard-side divertor plates is usually seen for all the discharges with  $R_{ax} = 3.6 \text{ m}$ . This strongly suggests that an enhanced particle recycling occurs at the inboard-side divertor region. The high-density helium neutral appeared around the inboard-side X-point is certainly ascribed to such an enhancement of the parti-

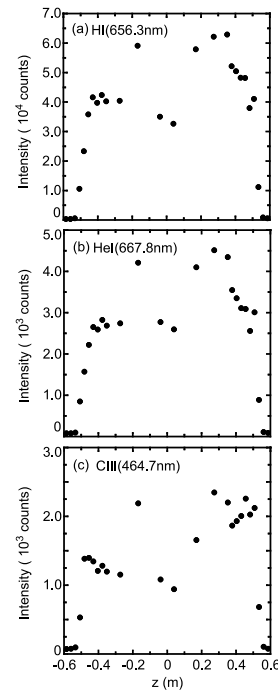


Fig. 5 Spatial distribution of (a) H I (656.3 nm), (b) He I (667.8 nm) and (c) C III (464.7 nm) in  $R_{ax} = 3.9 \text{ m}$  discharge.

Table 2 Local  $T_e$  and  $n_e$  evaluated from line ratios of He I  $I(667.8 \text{ nm})/I(728.1 \text{ nm})$ , He I  $I(728.1 \text{ nm})/I(706.5 \text{ nm})$  and H I  $I(656.3 \text{ nm})/I(434.1 \text{ nm})$  in  $R_{ax} = 3.9 \text{ m}$ .

$z$	HeI ratio ( $I(728.1 \text{ nm})/I(706.5 \text{ nm})$ )	$T_e$ (eV)	HeI ratio ( $I(667.8 \text{ nm})/I(728.1 \text{ nm})$ )	$n_e$ ( $10^{18} \text{ m}^{-3}$ )
(Inboard x-point) $z=0.38 \text{ m}$	0.23	23	3.7	6.0
(Outboard x-point) $z=-0.17 \text{ m}$	0.29	35	3.2	4.5
(bottom O-point) $z=-0.41 \text{ m}$	0.43	50	3.6	6.5

$z$	HI ratio ( $I(656.3 \text{ nm})/I(434.1 \text{ nm})$ )	$n_e$ ( $10^{18} \text{ m}^{-3}$ )
(Inboard x-point) $z=0.38 \text{ m}$	32.9	2.3
(Outboard x-point) $z=-0.17 \text{ m}$	38.6	2.5
(bottom O-point) $z=-0.41 \text{ m}$	45.7	4.8

cle recycling on the inboard-side divertor plates.

A similar measurement is also done for the  $R_{ax} = 3.9 \text{ m}$  configuration (see Fig. 1 (b)). Figure 5 (a) shows the same emission distributions as Fig. 3. In addition to the intensity peak observed around  $z = 0.3 \text{ m}$ , we see a new peak at  $z = -0.17 \text{ m}$ , which may appear owing to the strong particle recycling in the outboard side region.

Evaluation of  $T_e$  and  $n_e$  is attempted again and the results are listed in Table 2. In contrast to the  $R_{ax} = 3.6 \text{ m}$  case, the  $n_e$  around the inboard-side X-point becomes high. Taking into account the parameters and the observed distribution shown in Fig. 5 (b), the helium neutral density is roughly the same around the two X-points. The ion flux on the divertor plates also drastically changes, when the  $R_{ax}$  is shifted to  $3.9 \text{ m}$ . Therefore, the present result for

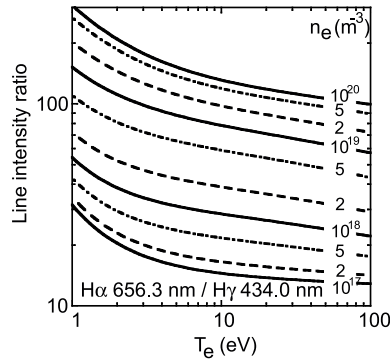


Fig. 6 Line intensity ratio of H I I(656.3 nm)/I(434.1 nm) calculated from C-R model simulation.

$R_{ax} = 3.9$  m is quite reasonable.

Finally, we try to evaluate the  $n_e$  using the intensity ratio of the H I 656.3 nm (H $\alpha$ ) and 434.1 nm (H $\gamma$ ) lines [7] to confirm the result from the helium intensity ratios. The CR-model result on the hydrogen is shown in Fig. 6. The intensity ratio mainly depends on  $n_e$ , but a weak  $T_e$  dependence is also seen. Then, the  $T_e$  values determined from the helium ratio is adopted for the analysis.

The obtained  $n_e$  values shown in Tables 1 and 2 are in fairly good agreement with those determined from helium ratio within an order. The difference may be caused by the slightly different emission locations for hydrogen and helium lines.

The  $n_e$  distribution determined with the neutral hydrogen line is quite similar to that determined with the helium lines. Since the intensity profile of the hydrogen line is also similar to that of the helium line as seen in Fig. 3 and Fig. 5, the same poloidal density inhomogeneity is again

suggested for the hydrogen atom.

## 4. Summary

Inhomogeneous poloidal distribution of the neutral emission intensity is observed from visible spectroscopy. In order to analyze the physical mechanism the edge temperature and density are evaluated from line ratios of He I and H I emissions. As a result, it is found that the poloidal inhomogeneity originates in the neutral particle density itself, but not in the electron density or temperature. It is the future subject to study the further detailed mechanism of the poloidally localized neutral density, which is extremely important for the improvement of the LHD performance. The visible system will be improved to measure more detailed profile in near future.

## Acknowledgements

The authors thank to all members of LHD experimental group for their technical support. This study was made in part under the financial support by the LHD project (NIFS06ULPP527).

- [1] M. Goto and S. Morita, Phys. Rev. **E 65**, 026401 (2002).
- [2] S. Morita, M. Goto *et al.*, Physica Scripta **T91**, 48 (2001).
- [3] B. Schweer, G. Mank, A. Pospieszczyk *et al.*, J. Nucl. Mater. **196-198**, 174 (1992).
- [4] M. Goto, JQSRT **76**, 331 (2003).
- [5] S. Masuzaki, T. Morisaki, M. Shoji *et al.*, Fusion Sci. Tech. **50**, 316105 (2006).
- [6] T. Morisaki, S. Masuzaki, M. Goto, S. Morita *et al.*, Contrib. Plasma Phys. **42**, 321 (2002).
- [7] T. Fujimoto and S.M. atsumoto, Nucl. Fusion **28**, 267 (1988).